Signatures of Bulk and Surface Arsenic Antisite Defects in GaAs(110)

R. B. Capaz, K. Cho, and J. D. Joannopoulos
Department of Physics, Massachusetts Institute of Technology, Cambridge, Massachusetts 02139
(Received 23 May 1995)

Scanning tunneling microscopy (STM) has recently been used in the study of *bulk* arsenic antisite defects in GaAs. In this work, we report extensive theoretical calculations of such defects in the vicinity of a GaAs(110) surface, which provide essential information for the interpretation of experiments. Defects display remarkably distinct properties depending on whether they are fourfold or threefold coordinated. The nature of "satellite peaks" observed in experiment is elucidated. We predict the conditions under which STM-measured properties will be faithful to the properties of the bulk defect.

PACS numbers: 61.72.Ji, 61.16.Ch, 71.55.Eq

In the past decade, scanning tunneling microscopy (STM) has emerged as an excellent technique for the study of semiconductor surfaces. Recently, in a seminal paper, Feenstra, Woodall, and Pettit (FWP) (the first paper of Ref. [1]) extended the range of potential applicability of STM to the study of *bulk* defects in semiconductors. In this context, a bulk defect can be loosely described as a point defect, which, albeit close enough to the surface to be detected by STM, still retains many of its bulk physical features (e.g., energy level, electronic structure, etc.). FWP obtained several types of STM images and inferred that they arise from isolated arsenic antisite defects (As on a Ga site) located at different depths below the GaAs(110) surface. In addition, some of the images exhibited intriguing "satellite peaks" located along the $[1\bar{1}\bar{2}]$ and $[\bar{1}1\bar{2}]$ directions relative to the central defect core. The origin of these peaks remained uncertain.

In this Letter we show how the predictive power of *ab initio* total energy methods can be used as an essential tool in the interpretation of the STM images. The interaction between defect and surface is expected to produce deviations from the bulk-like behavior. We show that these deviations are abruptly increased when the defect is located at the outermost surface plane [2]. There is a striking difference in terms of total energies, level positions, and local electronic structure between fourfold coordinated (below the surface plane) and threefold coordinated (at the surface plane) defects, which allows us to unambiguously define them as *bulk* and *surface* defects, respectively. We therefore predict the conditions under which most of the STM-measured quantities will be faithful to the properties of the bulk defect. The presence of the surface, however, produces also nontrivial changes in the *long-range* electronic structure of bulk defects. For instance, the nature of the satellite peaks observed by FWP is revealed as being *surface-enhanced* features of the defect-state wave function. Our results for the satellite positions with respect to the defect core also suggest that the [001] crystalline direction, as depicted in the STM images of FWP, is inverted. The new assignment is consistent with more recent experimental results.

The problem of a defect in the vicinity of a semiconductor surface is fairly complex and multifaceted. In order to maximize our understanding about the different aspects of the system while keeping the calculation tractable in terms of computer time, *ab initio* and empirical methods were used in a complementary manner. Three sets of calculations with well-defined goals were performed. In the first set, fully *ab initio* methods with ionic relaxation via Hellmann-Feynman forces were employed for four distinct values of the defect-surface distance in an 80-atom supercell. Our goals for this calculation were to investigate the energetics of the defect-surface system, to obtain local structural relaxations, and to study the short-range electronic structure. The second set consisted of a Keating-type valence-force-field study of long-range relaxations and a semiempirical tight-binding calculation of the energy levels in a much bigger (1536 atoms) supercell. Finally, in the third set of calculations, *ab initio* methods were again used to obtain a precise description of the nature of the satellite peaks in a 200-atom supercell with Keating-relaxed ionic positions.

(i) Ab initio calculations in a 80-atom supercell.— Our *ab initio* calculations are based on the local-density-function and pseudopotential approximations. Details are described elsewhere [3]. A plane-wave energy cutoff of 14 Ry was used. The 80-atom supercell consisted of a 2×2 GaAs(110) surface unit cell with 9 GaAs layers into the bulk and hydrogen saturation at the bottom. Seven GaAs layers were allowed to relax for each calculation. Reciprocal space sampling was restricted to the symmetrized special $\vec{k}$ point $(\frac{1}{4}, \frac{1}{4}, 0)$.

Table I shows total energy results for the arsenic antisite defect at the fourth layer, third layer, second layer, and first layer (surface layer) of GaAs(110). Notice the decrease in the total energy as the defect approaches the surface, which is indicative of an *attractive* defect-surface interaction. Moreover, notice the dramatic decrease in total energy as the antisite is moved from the second layer to the surface layer. This energy difference (about 1.8 eV) is too big to be explained in terms of "strain-release" effects solely. Therefore an abrupt change in the electronic

0031-9007/95/75(9)/1811(4)$06.00

TABLE I. *Ab initio* total energies (in eV) for the antisite defect located at different distances below the surface.

Fourth layer	Third layer	Second layer	First layer
0.00 (reference)	−0.15	−0.23	−2.07

structure of the defect must be occurring. The nature of this change is elucidated as we look at charge density contour plots for the occupied defect state in Fig. 1. In Fig. 1(a) (defect on the fourth layer) we see the familiar charge density signature of the bulk-like arsenic antisite defect [4], with *s*-like character on the central As atom and antibonding *p*-like character on the first neighboring As atoms (two of them are shown in the plane of the figure). In Figs. 1(b) and 1(c) (defects on the third and second layers, respectively), no significant change in the bulk-like charge density signature occurs. These three electronic states lie approximately at midgap, as the bulk defect does. In Fig. 1(d) we display the charge density plot for the defect at the surface layer. It is clearly a resonant As dangling-bond state, and it lies well within the valence band (notice the mixing with valence band states). This abrupt change in the electronic structure is a direct consequence of the change from fourfold to threefold coordination as the defect is placed at the surface layer. As we shall describe more quantitatively in the next section, this change will produce remarkable effects in the spectroscopy properties of the defect.

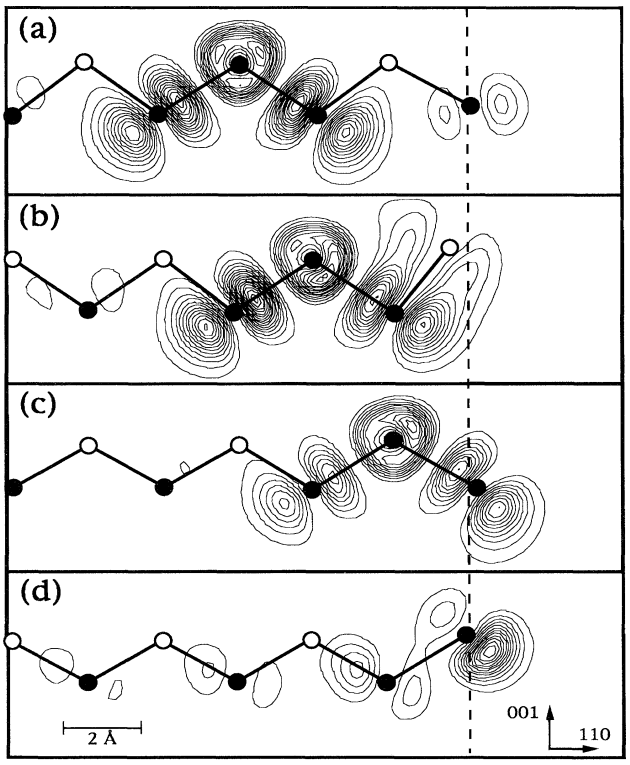

FIG. 1. Contour plots of electronic density for the antisite at the (a) fourth layer, (b) third layer, (c) second layer, and (d) first layer of the (110) surface. The dashed line denotes the position of the outermost As atoms in the pure surface. Black and white circles represent As and Ga atoms, respectively. Contours are evenly spaced by 0.005 electrons/Å^3, running from 0.005 electrons/Å^3 to the maximum density in each case.

(ii) Keating + tight-binding calculations in a 1536-atom supercell.—It is well known that long-range crystal relaxations around a defect core can be well described by simple valence-force-field models, such as the Keating model [5]. We used a slightly modified version of such a model that incorporates surface relaxation effects. Essentially, distinct values of model bond length and bond angle parameters were introduced for the surface bonds in order to describe the familiar "buckling" of the pure GaAs(110) surface. This model was then used to study the long-range strain relaxations of the surface in the presence of the antisite defect. It was conjectured by FWP that the presence of satellite peaks along the $[1\bar{1}\bar{2}]$ and $[\bar{1}1\bar{2}]$ could be explained by strain-related variations in the surface buckling. Our results do not support this interpretation. In Fig. 2 we plot the variation of the surface buckling angle (with respect to the pure surface) for the Ga-As bonds in the surface plane when the antisite is located at the second layer. Notice that variations in the surface buckling angle decay very rapidly with distance, so that the only bonds showing a significant change (approximately 10°) in the buckling angle are those linking the central As surface atom (which is "pushed away" by the antisite just below it) and its two Ga neighbors. All the other changes in the surface buckling are negligible, and this does not seem to be the correct mechanism for the appearance of the satellite peaks.

We took advantage of the large Keating-relaxed supercells in order to perform empirical tight-binding calculations of defect energy levels. Tight-binding methods have been sucessfully used to describe both surface electronic states in GaAs(110) [6] as well as the isolated As antisite

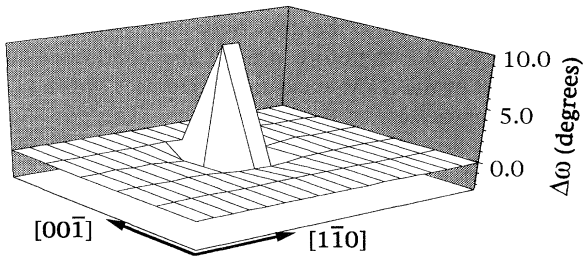

FIG. 2. Variations of the surface buckling angle ω for the surface Ga-As bonds. Each midbond point is represented by a mesh point. The zigzag bond pattern of the (110) surface is then mapped into a rectangular mesh. $\omega = 30°$ for the pure surface.

defect in GaAs [7]. We adopted the five-orbital sp^3s^* basis set introduced by Vogl, Hjalmarson, and Dow [8]. As suggested in Ref. [12], the s^*_{As}-p_{As} matrix element was tuned to reproduce the energy level position of the bulk As-antisite defect (E_v + 0.75 eV). Level positions for the defect at different distances from the surface were then calculated, and the results are displayed in Table II. Notice that the level positions remain essentially bulklike until the defect is located at the surface layer, when it then drops to about 0.4 eV below the valence band edge. These results should have profound consequences as far as STM spectroscopy is concerned. They imply that it is indeed possible to obtain an accurate description of bulk defect energy levels using STM, as suggested by FWP, as long as the defect is located *below* the surface layer. Furthermore, they predict that the surface defect will have very distinct spectroscopic signatures from the bulk ones. A defect level around E_v − 0.4 eV that would correspond to the antisite dangling bond has not been observed by FWP, however. Further investigation is needed to clarify this issue.

(iii) Ab initio calculation in a 200-atom supercell.— We now return to *ab initio* methods in order to investigate the origin and nature of the long-range satellite peaks observed in some of the images of FWP. Experimentally, these features appear to be more intense for defects located at the second layer. Therefore, this is the case we will focus on in our calculations. A 200-atom supercell (81 As, 79 Ga, 40 H) was used, corresponding to a 5 × 4 surface unit cell, 4 GaAs layers and hydrogen saturation on the bottom. Atomic positions were kept fixed at the Keating-relaxed values. A 14 Ry energy cutoff (45 767 plane waves) was imposed and Γ-point sampling was used. This calculation approaches the *ab initio* state of the art in terms of size, and it was performed in a parallel CM-5 computer. Simulated constant-current STM images were obtained within the Tersoff-Hamann approximation [9], which essentially implies that the tunneling current is proportional to the sum of local charge density contributions from all states encompassed by the applied bias voltage.

In Fig. 3 we show a theoretical STM image of the GaAs(110) surface in the vicinity of the antisite. The bias voltage is negative and small enough to only include contributions from the occupied midgap defect state. The theoretical image shows a remarkable similarity to experiment (see, for instance, Fig. 5 of FWP), but only if one assumes that the determination of the [001] crystalline direction is *inverted*. Indeed, a reevaluation of the assignment of the [001] direction of FWP (as determined by anisotropic etching on the same samples studied there) now leads to a consistent picture between theory and experiment [10]. Notice also the presence of the satellite peaks as distant "spotlike" features along the $[1\bar{1}2]$ and $[\bar{1}12]$ directions from the defect core (not $[1\bar{1}\bar{2}]$ and $[\bar{1}1\bar{2}]$ as stated by FWP). Interestingly, the satellites seem to be only part of a much larger ensemble of spotlike features on the STM image, with no special significance other than being considerably farther away from the defect core than the other spotlike features. This is probably the reason why they stand out on the experimental images, while the other peaks merge to the central peak due to the finite resolution of the STM tip. The nature of these spotlike features is elucidated in Fig. 4, where we perform a close comparison between theory and experiment by plotting theoretical charge density cuts (in a log scale) along with experimental cross-sectional cuts of the tip height variation. Several noteworthy features are found. First of all, it is clear that the defect wave function is more extended along the $[1\bar{1}2]$ and $[\bar{1}12]$ directions than along the [001] direction, an effect that was correctly captured by experiment [11]. It is also clear that this property is *reminiscent* of the bulk defect wave function, as we can see by looking at the charge density region that extends into the bulk. However, most of the spotlike features observed in the STM images, which appear in Fig. 4 as atomiclike orbitals sticking out of the surface atoms, *do not have a bulk counterpart at the atoms in the third*

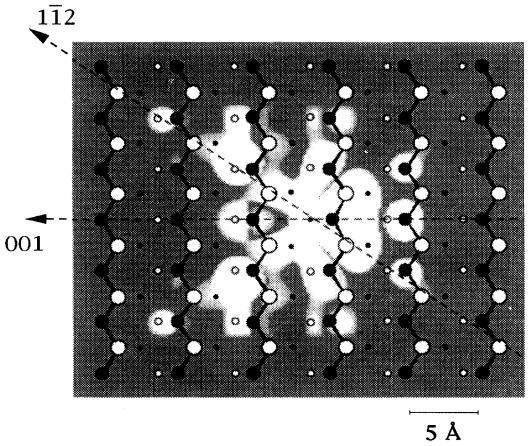

FIG. 3. Theoretical STM image of the GaAs(110) surface with the defect in the second layer. In order to simulate the image of the isolated defect (without the periodic repetition inherent to the supercell scheme), the image was properly "cut" and superimposed into a grey background. Contrast was enhanced to emphasize all image features. Dashed lines indicate the positions of cross-sectional cut planes of Fig. 4. Large and small circles represent first layer and second layer atoms, respectively (black for As and white for Ga). The constant local charge density is $\rho = 10^{-4}$.

TABLE II. Tight-binding energy levels (in eV, with respect to the valence band edge) for the antisite defect located at different distances below the surface.

Bulk	Fourth layer	Third layer	Second layer	First layer
0.75 (fitted)	0.77	0.77	0.74	−0.39

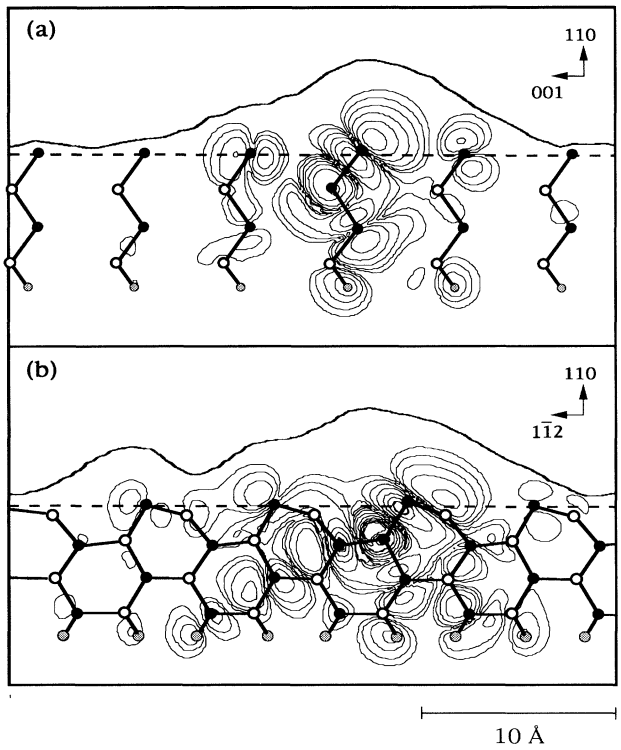

FIG. 4. Theoretical charge-density cuts and experimental tip-height cross-sectional plots along two different directions. The dashed line denotes the positions of the outermost As atoms in the pure surface. Black, white, and grey circles represent As, Ga, and H atomic positions [in (a)] or projections [in (b)] into the plane of cut. Theoretical contours are in a log scale $\rho = 10^{-n}$, n from 1.5 to 4 in units of 0.5. Experimental results correspond to Fig. 5 of FWP. The experimental corrugation was increased by a factor of 3 to allow a better qualitative comparison with theory.

layer. This shows how subtle the interpretation of the STM images is: Although it is correct to say that some bulk features are present, one cannot assume that the STM imaging process provides an unperturbed description of the bulk defect wave function. For instance, this is not true for the satellite peaks, which could be more correctly described as *surface enhanced* features of the bulk defect wave function.

In conclusion, we have performed an extensive theoretical investigation of the properties of an arsenic antisite defect in the vicinity of the GaAs(110) surface. Our results show that fourfold coordinated (below the surface layer) and threefold coordinated (at the surface layer) defects have remarkably distinct properties. It is therefore reasonable to classify them as bulk and surface defects, respectively. Theory has proved itself to be an indispensable tool, both in the interpretation of STM image features and in predicting which STM-measured properties can be interpreted as bulk properties. Energy level positions seem to be very robust properties, practically unchanged for all bulk defects. This makes STM spectroscopy of bulk defects a new and powerful technique to be further explored. STM imaging results, however, have to be interpreted with care. We have shown that some specific long-range features can be induced by the surface, even though the image has a general shape that is reminiscent from the bulk defect wave function.

R. B. C. is grateful to Conselho Nacional de Desenvolvimento Científico e Tecnológico (CNPq-Brazil) for providing financial support. We are especially grateful to Dr. R. M. Feenstra for providing us with experimental cross-sectional plots and other unpublished results. We also would like to acknowledge useful conversations with Dr. J. F. Zheng.

[1] R. M. Feenstra, J. M. Woodall, and G. D. Pettit, Phys. Rev. Lett. **71**, 1176 (1993); also see R. M. Feenstra, J. M. Woodall, and G. D. Pettit, Mater. Sci. Forum **143–147**, 1311 (1994).

[2] Similar behavior has been recently observed for silicon impurities in GaAs, see J. F. Zheng, X. Liu, N. Newman, E. R. Weber, D. F. Ogletree, and M. Salmeron, Phys. Rev. Lett. **72**, 1490 (1994).

[3] M. C. Payne, M. P. Teter, D. C. Allan, T. A. Arias, and J. D. Joannopoulos, Rev. Mod. Phys. **64**, 1045 (1992).

[4] J. Dabrowski and M. Scheffler, Phys. Rev. B **40**, 10391 (1989).

[5] P. N. Keating, Phys. Rev. **145**, 637 (1966); model parameters for GaAs were taken from J. L. Martins and A. Zunger, Phys. Rev. B **30**, 6217 (1984).

[6] E. J. Mele and J. D. Joannopoulos, Phys. Rev. B **17**, 1816 (1978).

[7] B. K. Agrawal, S. Agrawal, P. S. Yadav, J. S. Negi, and S. Kumar, Philos. Mag. B **63**, 657 (1991).

[8] P. Vogl, H. P. Hjalmarson, and J. D. Dow, J. Phys. Chem. Solids **44**, 365 (1983).

[9] J. Tersoff and D. R. Hamann, Phys. Rev. B **31**, 805 (1985).

[10] Anisotropic etching on the backside of the wafers using 1:4 HF:H_2O_2 revealed etch pits elongated along the [1$\bar{1}$0] direction (as opposed to the [110] direction normal to the cleavage face). With the long side of the etch pitchs corresponding to a V groove with Ga-terminated (111) planes, and knowing that the back side of the wafer is on the right-hand side of the STM images, it is directly determined that the Ga atoms in the surface zigzag chains point towards the right-hand side of the images (just like it is shown in Fig. 3 and contrary to that shown in Fig. 5 of FWP). [R. M. Feenstra (private communication)].

[11] This can be explained as a consequence of the directionality of the As-As bonds and the high connectivity of the (111) planes. However, it is a purely electronic effect, not strain related.

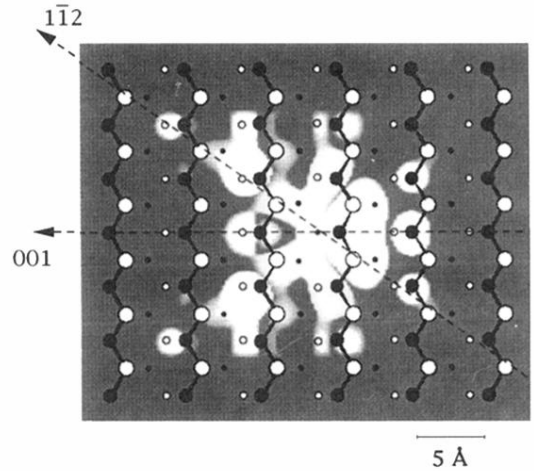

FIG. 3. Theoretical STM image of the GaAs(110) surface with the defect in the second layer. In order to simulate the image of the isolated defect (without the periodic repetition inherent to the supercell scheme), the image was properly "cut" and superimposed into a grey background. Contrast was enhanced to emphasize all image features. Dashed lines indicate the positions of cross-sectional cut planes of Fig. 4. Large and small circles represent first layer and second layer atoms, respectively (black for As and white for Ga). The constant local charge density is $\rho = 10^{-4}$.